

GolP: An Atomistic Force-Field to Describe the Interaction of Proteins With Au(111) Surfaces in Water

F. IORI,¹ R. DI FELICE,² E. MOLINARI,^{1,2} S. CORNI²

¹Department of Physics, University of Modena and Reggio Emilia, Modena, Italy

²INFN-CNR National Research Center on nanoStructures and bioSystems at Surfaces (S3),
Modena, Italy

Received 11 June 2008; Accepted 10 October 2008

DOI 10.1002/jcc.21165

Published online 25 November 2008 in Wiley InterScience (www.interscience.wiley.com).

Abstract: A classical atomistic force field to describe the interaction of proteins with gold (111) surfaces in explicit water has been devised. The force field is specifically designed to be easily usable in most common bio-oriented molecular dynamics codes, such as GROMACS and NAMD. Its parametrization is based on quantum mechanical (density functional theory [DFT] and second order Möller-Plesset perturbation theory [MP2]) calculations and experimental data on the adsorption of small molecules on gold. In particular, a systematic DFT survey of the interaction between Au(111) and the natural amino acid side chains has been performed to single out chemisorption effects. Van der Waals parameters have been instead fitted to experimental desorption energy data of linear alkanes and were also studied via MP2 calculations. Finally, gold polarization (image charge effects) is taken into account by a recently proposed procedure (Iori, F.; Corni, S. *J Comp Chem* 2008, 29, 1656). Preliminary validation results of GolP on an independent test set of small molecules show the good performances of the force field.

© 2008 Wiley Periodicals, Inc. *J Comput Chem* 30: 1465–1476, 2009

Key words: molecular dynamics; gold surfaces; force fields

Introduction

The capability of proteins to selectively recognize bare inorganic surfaces has a great importance in several fields, ranging from medicine to nanobioelectronics. This capability has been experimentally demonstrated by various groups (e.g.,^{1–3} just to cite a few). However, the available techniques to get surface-selective proteins are based on combinatorial approaches (cell surface and phage displays) that deliver a result but leave the reasons of such a result unknown. What are the reasons why a given sequence has a higher affinity for a given surface? Which factors (energetic, entropic, and morphological) are the most relevant? Answering to these questions is not only important from a fundamental science point of view, but opens the way to rational design of proteins able to selectively interact (or maybe not to interact) with a given inorganic surface.

The long-term aim of our research is to unravel by computational approaches the concepts that are at the basis of selective protein-surface interactions. To tackle this ambitious objective by computational methods, first one has to derive the proper tools to reliably describe *in silico* the system of interest.

Due to the complexity of a system composed by an inorganic surface, a protein (or a peptide) and water, a systematic approach based on quantum-mechanical *ab initio* techniques is

unfeasible, although possible for selected prototypical systems. On the contrary, a classical atomistic molecular dynamics (MD) study of the system seems the best compromise between computational accessibility and capability of correctly catching the physics of the system. The separation of the interaction energy that is inherent to classical force fields (FFs) is particularly convenient to interpret the computational results in terms of basic physico-chemical concepts such as electrostatics and polarization, dispersion forces, and entropic effects.

Although the FFs to describe proteins in water have been developed for a long time, and are still being improved (e.g., inclusion of electronic polarization effects), at present FFs specifically designed to treat protein-surface interaction are lacking. Parameters used in published atomistic protein-surface MD simulations were mostly based on reasonable guesses (see, e.g.,^{4–11}) possibly verified *a posteriori*.

Correspondence to: S. Corni; e-mail: stefano.corni@unimore.it

Contract/grant sponsor: EU under the Sixth Framework Program, project PROSURF; contract/grant number: FP6-NEST- 028331.

Contract/grant sponsor: Computer time from the CINECA supercomputer center.

The present work describes our approach to design a classical FF (named *GolP* FF, Gold-Protein FF) for the interaction of biomolecules (including, but not limited to, proteins) and the Au(111) surface. We have chosen this surface for different reasons:

- it has been the target surface for one of the best characterized surface-specific peptide (the gold-binding peptide [GBP]^{12–14});
- it has been the subject of several experimental studies on small molecule adsorption in well controlled conditions^{15–17} (which enables the extraction of parameters and a preliminary validation of the FF);
- it is stable also in contact with air and water (although it can be easily contaminated by hydrophobic molecules), and its typical $22 \times \sqrt{3}$ reconstruction is on the one hand well-characterized (also in water) and on the other hand does not profoundly affect the Au(111) reactivity;
- it is important for nanobioelectronics applications, since it represents the most used substrate for creating contacts of nano-objects with the macroscopic world; and
- it is used in optical detection systems for protein materials, such as the widely employed surface plasmon resonance (SPR) technique.

Although no FF specifically devised for protein-Au(111) interactions is available, different classical FFs have been proposed in the literature to describe the interaction of molecules with gold surfaces. In particular, the most common target system of such FFs was alkylthiol self-assembled monolayers (SAM) on gold. We can grossly separate such FFs in two groups:

- Surface potentials: those using potential functions with no direct reference to the atomic structure of gold, i.e., the FFs are a function only of the distance of the molecule from the surface;
- Atomistic potentials: those considering an atomistic description of the solid (i.e., the FF is a sum of functions of the distances between the gold atoms and the molecules). In this case, the surface may be rigid (gold atoms are forced to occupy their equilibrium position) or mobile (the positions of gold atoms evolve during the MD under a proper Au-Au FF).

(a) To describe a monolayer of alkyl thiol chains on Au(111), Hautman and Klein used a 12-3 Lennard-Jones (LJ)-like potential that depends on molecule atom-gold surface distance. LJ parameters for the alkyl chains have been estimated by the adsorption energy of Kr on Ag(111), while the adsorption energy of methylthiol was used for LJ parameters of S and for harmonic Au-S-C angle-terms.¹⁸ In following studies of analogous systems, a periodic corrugation potential for S was added to force chemisorption in high-symmetry surface sites.^{19,20} Pertsin and Grunze²¹ modified this FF by using a harmonic corrugation term for S with parameters fitted on quantum-mechanical calculations.²² The Hautman and Klein FF was also used in more recent studies of SAMs.^{23,24}

Based on a previous proposal by Spohr,²⁵ Dou et al.²⁶ developed a FF for water-gold interactions based on a sum of Morse potentials that are functions of the O-surface and H-surface distances, weighted by a surface corrugation potential.

Qian et al. developed another gold-molecule FF to study cyclodextrin derivatives on Au(111).²⁷ They used a 10-4 LJ potential between the molecule and each gold layer. Parameters for this potential were obtained by mixing rules from the Universal Force Field (UFF).²⁸ It is worth mentioning that LJ parameters for gold in such a FF were actually derived for Au(III) complexes, not for solid gold. Parameters for the surface corrugation potential were the same of Pertsin and Grunze.²¹ Qian et al. also analyzed the effects of image charge interactions (i.e., gold-polarization effects) for their specific system, although they did not include them in the simulation. For a more comprehensive discussion of approaches to include image effects in classical MD simulations of molecules on metals, we refer to 29. The FF by Qian et al. was also used by Braun et al.⁹ to simulate the gold binding protein¹² on Au(111) in water.

Finally, a FF to describe gold-water and gold-benzene interactions has been developed by Schrevelndijk et al.,³⁰ who employed 10-4 LJ potentials, with parameters fitted to plane-wave density functional theory (DFT) results.

(b) The surface potential by Hautman and Klein was transformed to an atomistic potential with rigid surfaces by Tupper and Brenner (who used atom-atom 12-3 LJ potentials)³¹ and to an atomistic potential with mobile surfaces by Mahaffy et al.³² (who used 12-6 LJ). In the latter study, the Au-Au atomic potential by De Pristo and co-workers is used.³³ Gerdy and Goddard³⁴ studied the packing of alkylthiols SAMs on the Au(111) rigid surface by a modified DREIDING FF.³⁵ In a subsequent work of the same group³⁶ MD parameters for S-Au interactions were derived by *ab initio* calculations, while the van der Waals (vdW) interactions were represented by atom-atom 12-6 LJ potentials, with parameters from the UFF. Afterwards, SAMs of rotaxanes on Au(111) were studied³⁷ and new parameters for Au-S interactions were derived from *ab initio* calculations; the vdW surface-molecule interactions were described by exp-6 potential with DREIDING/UFF parameters.³⁷ The gold surface was mobile, with Au-Au interactions described by exp-6 potentials with parameters fitted to reproduce experimental bulk properties. The same FF, with rigid surface, has been also recently used by others.³⁸

In a series of articles Zerbetto and co-workers³⁹ developed an organic molecule-gold surface FF. The gold-surface interaction was described via electrostatic and Born-Mayer potentials. Charges on gold and on the molecule were derived by the QEeq charge equalization method.⁴⁰ The parameters of the Born-Mayer potentials were fitted to experimental data on alkanes, alkenes, and nucleobases on gold, achieving a good agreement with experimental adsorption energies. The Au-Au interaction was described by the glue model.⁴¹ Recently, the effects of potentials applied to gold were also modeled.⁴²

Leng et al.⁴³ used 12-6 LJ atom-atom potentials with parameters from the UFF, combined with electrostatic partial-charge interactions from Mülliken population analysis (including partial charges on gold atoms) of *ab initio* calculations. The Au(111) was held rigid.

Bizzarri et al.⁴⁴ and Setty-Venkat et al.⁴⁵ applied an atomistic version of the Qian et al. potential²⁷ to study mutated plastocyanin and azurin (blue-copper proteins) anchored via cysteine on rigid Au(111) in water.

Finally, Piana and Bilic⁴⁶ developed a FF for gold-molecule interactions based on quantum-chemical (MP2) calculations on Au₄ clusters and small model molecules, which were used to derive atom-atom 12-6 LJ parameters. The FF has been applied to study DNA nucleobases monolayers on Au(111), obtaining interaction energies in agreement with the available experiments.

FFs devised for alkylthiols on gold may be applicable to proteins when the interaction with the surface is dominated by covalent Au-S bonds, but they cannot convincingly describe protein-surface systems where the adhesion mainly comes from secondary interactions. The factors that hinder the use of the FFs mentioned so far for generic proteins are:

- The poorly understood nature (chemi- versus physisorption) of the interaction of the natural amino acids with Au(111), with the exception of Cys. Such a nature may even affect the form of the FF.
- The unavailability of van der Waals parameters for the interaction between gold and the several atom types of proteins. Even when the validity of mixing rules is assumed, reliable parameters for Au are lacking.
- The neglect of gold polarization (or image charge) effects, which is not justified *a priori* for large, low-permittivity adsorbates.²⁹
- Finally, a practical reason not to be underestimated is that most FFs are not compatible with efficient bio-oriented MD codes, thus hampering long simulations on realistic systems.

Our FF has been designed with all these issues in mind. It is based on an atomistic description of the gold surface, both to allow easy compatibility with existing bio-oriented MD codes (where surface-like potentials are not always available) and, in perspective, to enable the description of a mobile gold surface. However, in this first version of our FF the gold surface is kept rigid. 12-6 LJ site-site potentials are used to describe the molecule-gold interaction. In addition, the gold polarization is taken into account according to a recently proposed protocol.²⁹ To determine the nature of adsorption of natural amino acids, a systematic DFT survey has been performed. Parameters for our FF have been derived by combining experimental data (whenever available) and calculations.

The rest of the article is organized as follows: in “Developing the FF,” we shall detail the form of the FF and the way the FF parameters have been derived by experiments and calculations; then, in “Preliminary test of the FF” we shall present some initial tests to demonstrate the usefulness of the FF. Finally, conclusions are drawn.

Developing the FF

The development of a FF for a gold surface should take into account some peculiarities originating from the metallic character of gold. On one hand, the FF must be designed to include the polarization of gold because of the charge density of the adsorbed molecules (image interactions). On the other hand, gold may receive dative bonds from adsorbed molecules, originating chemisorbed species. The FF for gold-protein interactions, thus, has the following form:

$$E_{\text{int}} = E_{\text{image}} + E_{\text{chemisorb}} + E_{\text{vdW}} + E_{\pi} \quad (1)$$

i.e., the total interaction energy (E_{int}) is decomposed in an image interaction contribution (E_{image}), one accounting for chemisorption ($E_{\text{chemisorb}}$), a van der Waals interaction term (E_{vdW}), and finally a term specific for conjugated (π) systems (E_{π}). Note that this FF does not include intra-surface (i.e., gold-gold) interaction terms, since we assume a rigid gold surface. The $22 \times \sqrt{3}$ reconstruction is neglected for the moment. The perturbation of the local structure of Au(111)-(1 × 1) by this reconstruction is quite small.

The strategy followed for parameterizing the Au(111)-protein interaction is the following:

1. Addressing the problem of how to include the image term (E_{image}) in the FF. This step has been accomplished in²⁹ and it will be only summarized here.
2. Plane waves (PW)-DFT calculations of small molecules representing the natural amino-acids on Au(111). Results: identification of molecules showing chemisorption character; parameterization of such interactions ($E_{\text{chemisorb}}$); verification of the FF form suitability to reproduce DFT results.
3. Parameterization of vdW terms on experiments on alkanes. Check of the vdW parameters transferability (i.e., validity of mixing rules) based on post-Hartree Fock (Möller-Plesset perturbation theory at the second order, MP2) computational results. Results: parameters to be used, via a mixing rule, for generic gold-atom vdW interaction (E_{vdW}).
4. Refinement for conjugated molecules, based on experimental results. Results: parameters to be used, via mixing rule, for the interaction between atoms of π systems and gold (E_{π}).

1. Image interactions: Although different proposals exist in the literature to include such interactions in a classical FF,^{47–49} their use requires to work on the source code of the MD program of choice. We conceived and tested²⁹ a method that does not require any coding; it exploits the standard input structure of any bio-oriented software such as GROMACS⁵⁰ and NAMD⁵¹ (codes on which this method has been tested). The basic idea of the method is to reproduce the electronic metal polarization effects in classical terms by replacing each gold atom with a dipole made up by two, opposite charges. The two charges of each dipole are connected to each other by a rigid rod free to rotate (see Fig. 1). A charge external to the metal (i.e., a partial atomic charge placed on a nearby protein atom) forces the rod towards an energetically preferential orientation, and the average dipole moment of the rod (that is free to rotate around one of its ends) changes from 0 (the rod explores all the orientation with the same probability) to a given finite value. A spring (also known as “shell” or “Drude”) model^{52,53} has been also unsuccessfully tested by us.²⁹ We found that the rod model well reproduces classical electrostatic results (that, in turn, are good approximations of quantum results in the distance range we are interested in⁴⁷), even those involving the three-body nature (charge-metal-other charge) of the image term. In addition, with a simple model example, we demonstrated²⁹ that image interactions are indeed important in the description of molecules on

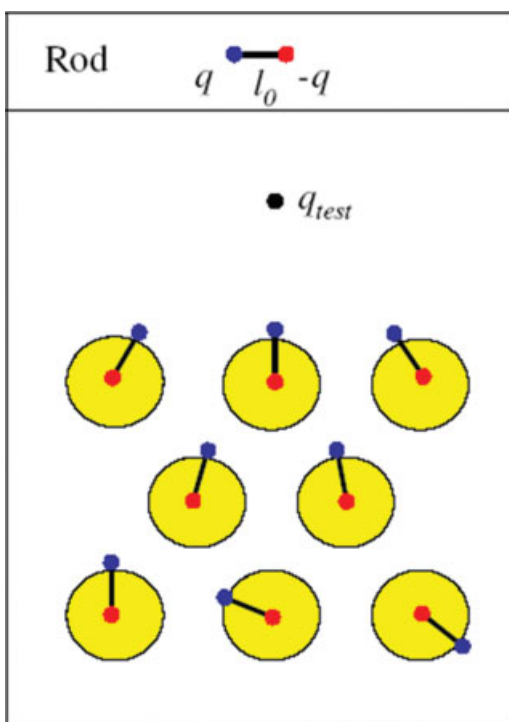


Figure 1. Scheme of the model to account for image interactions.

metal surfaces. This means that neglecting such terms (as always done in previous studies of protein-surface interactions) is, in general, unjustified and leads in some cases to major shortcomings.

2. Chemisorption: To address the issue of the nature of the interactions between Au(111) and the natural amino acids, we have performed a systematic computational study. In particular, we have used PW-DFT calculations in the periodic supercell approach. A slab of four gold layers represented the Au(111) surface. In principle, we should place each one of the 20 amino acids on gold, possibly starting by different conformations and orientations of the amino acid, not to mention the different protonation states to be considered. Such a huge study has the hallmark of unfeasibility. In addition, it would be highly redundant: for amino acids bearing a side-chain with a weak interaction with gold (e.g., glycine, alanine, leucine, etc.), we would reduce to study several times the adsorption of amino acid termini ($-\text{NH}_3^+$ and $-\text{COO}^-$). Thus, we adopted a chemical point of view, and decomposed each amino acid in simple molecules representative of their chemical functionality. The studied molecules and the related amino acids are reported in Table 1. All the studied molecules may in principle disclose interactions with the surface different from pure vdW terms. Despite the well-known shortcomings of current exchange-correlation (xc) DFT functionals to describe vdW interactions, the other kinds of interaction (e.g., bond-like) can be accurately grasped by a DFT investigation. VdW terms require a different approach (see

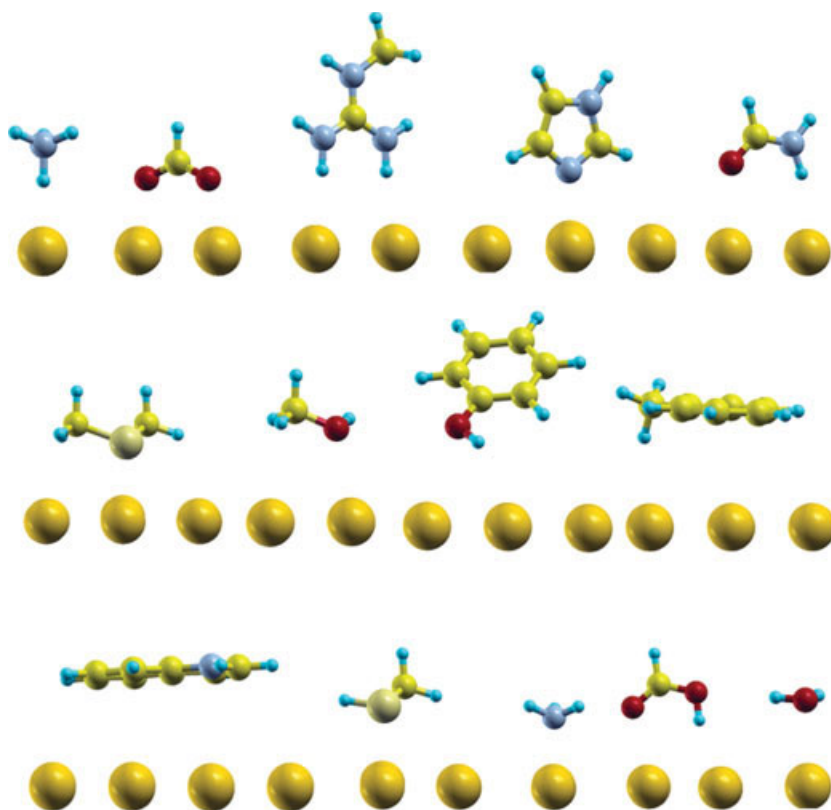


Figure 2. Lateral view of the adsorption geometry obtained by DFT calculations for all the 14 molecules in Table 1. Only the uppermost gold layer is shown in the figure.

Table 1. List of Molecules Studied on Au(111) by DFT Calculations and Related Amino Acids (AA).

Molecule	AA
CH ₃ OH	SER,THR
Imidazole	HIS
Indole	TRP
CH ₃ SH	CYS
CH ₃ SCH ₃	MET
Phenol	TYR
Toluene	PHE
Methylguanidinium	ARG
NH ₄ ⁺	LYS, N-TER
HCOO ⁻	GLU, ASP, C-TER
HCONH ₂	GLN, ASN
NH ₃	LYS, N-TER
HCOOH	GLU, ASP, C-TER
Water	

below). Simple alkane molecules (e.g., methane to represent alanine side chain), instead, were not considered at this stage because they undergo solely vdW interactions with the surface: consequently, the DFT treatment is inadequate.

For each of the 14 studied molecules, we chose a few probable starting geometries and optimized (relaxed) their structure on Au(111). The PBE xc functional⁵⁴ was employed throughout this study. For all the molecules we used a $2\sqrt{3} \times 3$ supercell with four atomic layers of gold, amounting to 48 atoms of gold (i.e., at least 500 explicit e⁻) in the cell. Further computational details are given in the appendix. For water, results are in agreement with the previous study by Michaelides et al.⁵⁵ The resulting DFT geometries are summarized in Figure 2. Although the computational effort is much smaller than the study of entire amino acids, it still remains challenging given the large amount of systems to be taken into account in a comprehensive study for natural amino acids.

The nature of the interaction between a molecule and gold could be determined, in principle, by the analysis of the electronic structures (projected density of states, PDOS, and orbital isosurfaces). Doing this analysis for each molecule would have been too time-consuming. We have thus screened the results by analyzing in the first instance the resulting interaction energy, the height difference between Au and the closest molecular heavy atoms (see Table 2) and the molecular orientation.

From our analysis, we concluded that four molecules could be chemisorbed to some extent, i.e., imidazole, NH₃, CH₃SH and CH₃SCH₃. This did not come as a surprise, since the interaction of them (or similar molecules) with gold is known to be stronger than simple physisorption. Although the electronic structure of NH₃ on gold has already been studied by DFT⁵⁷ (not to mention CH₃SH), imidazole and CH₃SCH₃ were not equally well characterized. We thus proceeded to a detailed electronic structure characterization (58 and Iori, F.; Corni, S.; Di Felice, R. in preparation), which indeed showed the typical signatures of a weak chemisorption of these molecules on gold. Such signatures are represented by the presence of bonding and antibonding orbitals below and above, respectively, the Fermi

energy as depicted in Figure 3. Note, however, that some antibonding orbitals appear also below the Fermi level.⁵⁸

A specific remark must be done for CH₃SH: it is well-known that thiols in general, and Cys in particular, adsorb on Au(111) via the S atom, by releasing H. We decided to include in our FF the parameters for the interaction of the undissociated -SH group with gold. In this way, an MD simulation of Cys-containing protein will give physical results on the possibility for the Cys molecule to come into close contact with the surface, which represents the step preliminary to S-H bond-dissociation and consequent strong chemisorption. Description by classical MD of the whole process (encounter and bond dissociation) would require a reactive FF,^{59,60} whose use is presently hindered by the high computational cost.

In terms of parameterization, the chemisorption interaction between gold and imidazole/NH₃/CH₃SH/CH₃SCH₃ should be accounted for by specific terms of the FF. In particular, we need potentials that allow dissociation of the gold-molecule bond (i.e., a harmonic term is not appropriate). The Morse potential term is available in some bio-oriented codes (GROMACS), but it is neither generally implemented, nor computationally efficient. Since energies for these molecules are quite small, we decided to verify if a LJ potential with proper parameters could reproduce the adsorption energies and geometries. We found that the answer is indeed positive, but to detail our findings it is necessary to first describe the form used for vdW interactions. This is done in the next section.

3. VdW interactions: The calculations on molecules on gold discussed so far were also the starting point to complete the parameterization of our FF. In principle, one could use interaction energies and minimum-energy geometries to find the parameter that, at this point of our discussion, still remains undetermined. However, it is well-known that current xc functionals (including PBE) do not properly account for long-range van der

Table 2. Interaction Energies E_{int} and Minimum Heavy Atoms Relative Height d for the Studied Molecules on Gold.

Molecule	E_{int} (kJ/mol)	$d(\text{\AA})$
Ammonium	-107.8	3.2
Formate	-134.6	2.3
Methylguanidinium	-76.0	3.5
(c) Imidazole	-45.6	2.3
Formamide	-20.9	2.6
(c) Dimethylsulfide	-46.6	2.6
Methanol	-12.5	2.8
Phenol	-8.8	3.6
Toluene	≈0.0	3.7
Indole	-11.3	3.5
(c) CH ₃ SH	-39.3	2.6
(c) NH ₃	-43.1	2.4
HCOOH	-13.6	3.0
Water	-12.1	2.8
(c) Cysteine ^a	-190	2.5

Chemisorbed molecules are marked with (c).

^aResult for chemisorption with homolytic dissociation of the Au-S bond, after [56].

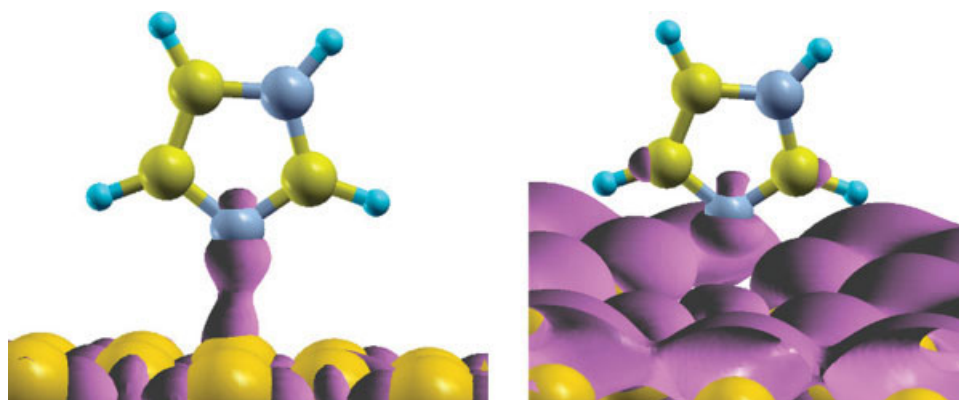


Figure 3. Bonding and anti-bonding orbitals with σ -character at -4.45 eV and $+0.75$ eV, respectively, w.r.t Fermi energy (after⁵⁸).

Waals interactions. In fact, for all the weakly polar molecules (phenol, toluene, indole) we hardly found an energy minimum close to the surface. We thus reverted to available experimental energy data on linear alkane adsorption on Au(111).¹⁴ We must first specify the form of the vdW FF. To keep our description coherent with bio-oriented FFs, we originally decided to describe E_{vdW} via an atomistic 12-6 LJ potential between each atom of the molecule and each gold atom on the surface, in the form:

$$V_{\text{LJ}}(r_{ij}) = 4\epsilon_{ij} \left(\left(\frac{\sigma_{ij}}{r_{ij}} \right)^{12} - \left(\frac{\sigma_{ij}}{r_{ij}} \right)^6 \right) \quad (2)$$

Unfortunately, this potential favors adsorption of atoms in the hollow site of the Au(111) surface (see Fig. 4), that does not agree with the results of our DFT calculations (even for non-chemisorbed species) and known results for rare-gas adsorption on noble metals,^{61,62} both pointing to the on-top adsorption site as the most favorable one. Driving the adsorption to the hollow instead of the on-top site has geometrical consequences, since the corresponding 2D lattices are different. In fact, the on-top sites are arranged after an hexagonal lattice with one site per

primitive cell, whereas the hollow sites occupy an hexagonal lattice with a basis of two sites per primitive cell (neglecting the influence of internal Au layers). The resulting patterns (see Fig. 4) cannot be superimposed by any roto-translation and are physically inequivalent. Adsorption of molecules with an intrinsic internal periodicity (such as linear alkanes) gives a different mismatch on the two lattices and, thus, different trends as a function of chain length.

To bypass this problem and keep an atomistic LJ description, for each real gold atom on the Au(111) surface we introduced two LJ virtual sites (VS) that occupy the hollow site (see Fig. 4). No LJ interaction was assigned to the original surface gold atoms, while no VS was used to replace gold atoms beneath the surface. With the expedient of VS, we could drive the adsorption of atoms to the on-top site. The position of the VS is also physically sound, since the density of free-electrons (the most effective in generating vdW interactions) in real metals is higher in the hollow site than on the lattice atoms.

To proceed with parameterization of this LJ interaction, we had to choose first a FF for the molecule. In fact, this fixes the mixing rule to obtain LJ parameters σ_{AB} , ϵ_{AB} for a generic couple of atoms A-B. It also fixes the values of σ_{AA} , ϵ_{AA} for each A. We decided to use the OPLS/AA FF (and coherently SPC for

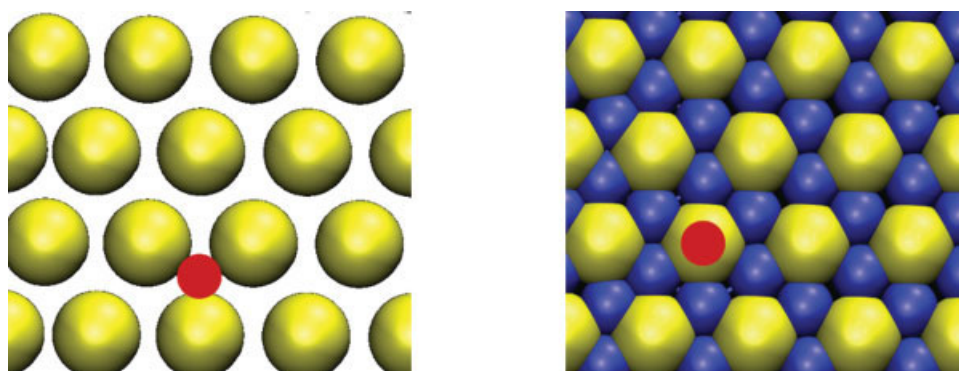


Figure 4. Using the real gold atoms as LJ interaction site drives adsorption in the hollow position (left panel), while the use of VS (in blue) drives adsorption on-top (right panel).

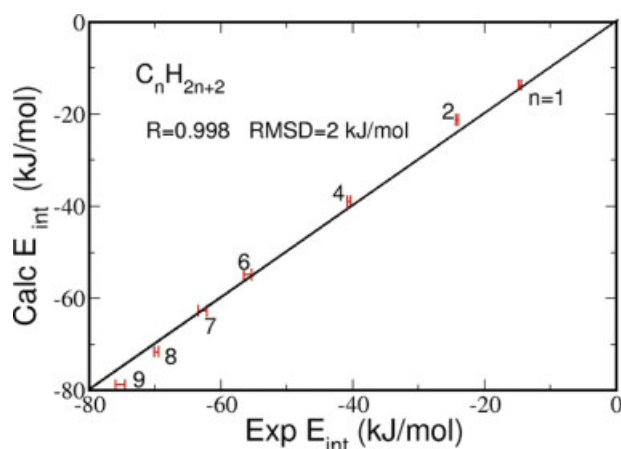


Figure 5. Interaction energies between Au(111) and alkanes as calculated via the developed FF (“Calc- E_{int} ”) and taken from the experiment (“Exp- E_{int} ”). [Color figure can be viewed in the online issue, which is available at www.interscience.wiley.com.]

water),⁶³ that gives a good description of proteins and is also parameterized for small molecules, as the ones studied by our DFT calculations.

We have verified that the LJ potentials from gold atoms beneath the surface give a small and smooth contribution to the overall vdW interaction between the gold slab and the adsorbed molecules. This makes unnecessary to precisely discriminate between LJ parameters of VS and bulk Au atoms, thus we have assumed $\sigma_{\text{VS-VS}} = \sigma_{\text{Au-Au}}$ (here Au is to be meant as the gold atoms not on the surface) and $\epsilon_{\text{VS-VS}} = \epsilon_{\text{Au-Au}}$. Then, we proceeded to obtain the parameters $\sigma_{\text{Au-Au}}$ and $\epsilon_{\text{Au-Au}}$ that best reproduce the experimental alkanes-Au(111) interaction energies (electrostatic interaction, although small, is taken into account with the rod model previously described). We found that $\sigma_{\text{Au-Au}} = 3.2 \text{ \AA}$ and $\epsilon_{\text{Au-Au}} = 0.65 \text{ kJ/mol}$ allow reproducing the experimental results¹⁵ extremely well ($R =$

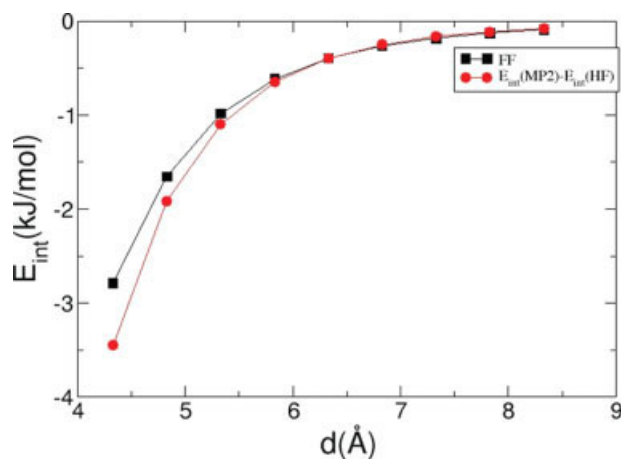


Figure 6. Interaction energies between CH_4 and Au_4 as a function of the distance between C and the Au_4 plane. [Color figure can be viewed in the online issue, which is available at www.interscience.wiley.com.]

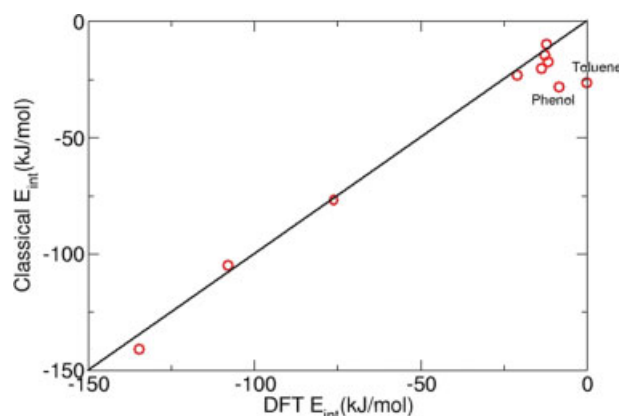


Figure 7. Classical vs. DFT interaction energies for physisorbed molecules. Classical results include a short-range energy contribution described via specific LJ parameters, different from that used for Figure 8. [Color figure can be viewed in the online issue, which is available at www.interscience.wiley.com.]

0.998 $\text{RMSD} = 2 \text{ kJ/mol}$, see Fig. 5), at a similar level of more flexible FFs previously described in the literature.³⁹ Considering that the geometry mismatch between alkanes and Au(111) is important in determining the interaction energy, this good agreement backs up the choice of introducing VS.

At this point we had to check the transferability of the generated parameters. In particular, it is very important that the FF gives a balanced description of the gold-molecule versus gold-water interactions, since the adsorption of a protein on a surface is actually a competition between the protein and water for that surface. Unfortunately, we are not aware of experimental interaction energies for water-Au(111) systems, although Kay et al.⁶⁴ gave an upper limit of 43.9 kJ/mol . We thus reverted to QM calculations able to include long-range dispersion interactions. It was reported before⁴⁶ that MP2 calculations done by representing the flat surface with a model Au_4 cluster (see appendix for calculation details) give LJ parameters that well reproduce the

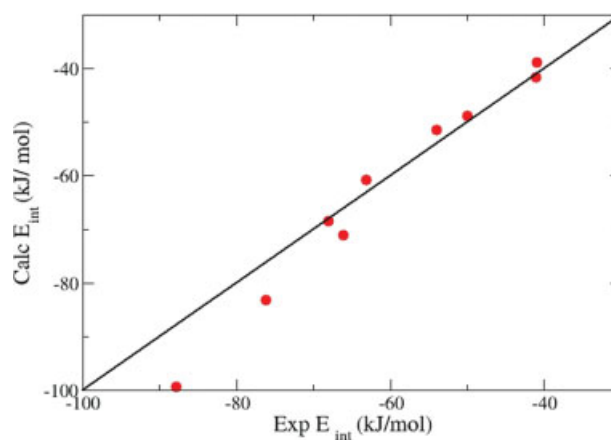


Figure 8. GolP vs. experimental interaction energies for a test set of molecules on Au(111). [Color figure can be viewed in the online issue, which is available at www.interscience.wiley.com.]

experimental interaction energy for the adsorption of DNA nucleobases on Au(111). Thus, we have first checked (for methane) if this level of calculation gives the same LJ parameters that we obtained by fitting experiments. We used the difference $E(\text{MP2})-E(\text{HF})$ as an estimate of the dispersion energy. As shown by the classical vs quantum results of Fig. 6, the MP2 calculations indeed agree with the classical results employing exp. fitted parameters. Then, we calculated the dispersion contribution for water-Au₄ interaction via the same MP2 approach, and we found again a good agreement between these results and that obtained by our experimental derived parameters and mixing rule (data not shown). Thus, our experimental parameters are transferable between two quite different molecules, methane and water. Although this does not prove transferability in general, it confirms that apolar molecule-gold versus water-gold dispersion interactions are well-balanced. Comparison with experiments will be the definitive benchmark for our parameters.

Let us come back now to the problem of choosing special LJ parameters for chemisorbed species to effectively reproduce their interaction energies and geometry on Au. The form of the vdW contribution to the FF is that just discussed. To minimize the number of parameters, we chose to use specific $\sigma_{\text{A-Au}}$ and $\epsilon_{\text{A-Au}}$ values only for the atoms A directly involved in the bond with the surface, i.e., N for imidazole/NH₃ and S for CH₃SH/CH₃SCH₃. The DFT interaction energy includes, beside chemisorption, other contributions coming from electrostatic (including the gold-molecule mutual polarization) and short-range xc effects that partially mimic, with the wrong distance dependence, the effects of dispersion interactions at small distances. In adjusting the chemisorption specific parameters, we should also take care of these other contributions. Gold polarization is taken into account by the rod model discussed above. For all the remaining interactions, we exploited a LJ potential, based on σ_{AuAu} , ϵ_{AuAu} values that best fit the DFT results of the non-chemisorbed molecules. The use of effective LJ parameters to fit PBE results does not imply that PBE is able to describe long range attractive interaction. We simply need a practical way to decouple in the classical FF the chemical-bond interaction occurring between N_{His}-Au or S_{Cys/Met}-Au and the other short-range contributions present in DFT calculations. The results of this fitting are reported in Fig. 7.

The good quality of the fitting is a proof of the valuable form chosen for the classical FF, which is able to fit several DFT calculations with only two adjustable parameters. Not only energies are good, but also geometries: we have always obtained a qualitatively equivalent geometry in DFT and classical calculations, and the Root Mean Square Deviation (RMSD) between the molecule-metal distances calculated by DFT or classical FF is 0.3 Å. Remarkably, during this fitting procedure, we noted that some of our minimized DFT structures were different from the classical ones, and by re-running the DFT calculations from the classical structure, we obtained a more stable minimum energy structure, coherent with the classical result (this happened for NH₂CHO, methylguanidinium and ammonium).

With this DFT-derived σ_{AuAu} , ϵ_{AuAu} at hand, we found $\sigma_{\text{N-Au}}$ and $\epsilon_{\text{N-Au}}$ values for imidazole and NH₃, and $\sigma_{\text{S-Au}}$, $\epsilon_{\text{S-Au}}$ values for CH₃SH and CH₃SCH₃. These values are reported in Table 3, together with the DFT versus classical interaction energies and molecule-metal distances. Remarkably, $\sigma_{\text{S-Au}}$, $\epsilon_{\text{S-Au}}$ values for

Table 3. LJ Parameters for Chemisorbed Molecules (σ in Å, ϵ in kJ/mol) and Relative FF and DFT Interaction Energies ($E_{\text{FF/DFT}}$ in kJ/mol) and Minimum Gold-Molecule Quote Difference ($d_{\text{FF/DFT}}$ in Å).

Molecule	$\sigma_{\text{SAu}}/\epsilon_{\text{SAu}}$	$\sigma_{\text{NAu}}/\epsilon_{\text{NAu}}$	$\sigma_{\text{HAu}}/\epsilon_{\text{HAu}}$	E_{FF}	E_{DFT}	d_{FF}	d_{DFT}
Imidazole	—	2.75/1.6	—	-46.1	-45.6	2.3	2.3
NH ₃ ^a	—	2.75/1.6	3.05/0.5	-45.1	-43.1	2.35	2.35
CH ₃ SCH ₃	2.9/2.7	—	—	-45.6	-46.6	2.7	2.6
CH ₃ SH	2.9/2.7	—	—	-39.7	-39.3	2.64	2.59

FF results have been obtained with σ_{AuAu} and ϵ_{AuAu} fitted from DFT results.

^aExp. adsorption energy: -42 kJ/mol [64].

CH₃SH and CH₃SCH₃ are identical. We should also mention that for NH₃, we had to define specific $\sigma_{\text{H-Au}}$, $\epsilon_{\text{H-Au}}$ parameters (in OPLS/AA, polar H has $\epsilon_{\text{H-H}} = 0$) to reproduce the DFT global minimum structure. In general, we found that polar H tends to be too close to the gold surface. The DFT value and the FF one are very close to the experimental estimate of the adsorption energy, -42 kJ/mol.⁶⁴

4. π systems: Our GGA calculations on aromatic molecules on Au(111) did not evidence any special interaction, apart from the weakly chemisorbed imidazole. However, when we tested our FF by calculating the adsorption energies of conjugated systems (namely ethene, 1,3-butadiene, benzene) on gold, we got a disappointing result: the interaction energies were -19 kJ/mol, -35 kJ/mol, and -43 kJ/mol for ethene, 1,3-butadiene and benzene, respectively, while the experimental energies¹⁵ are -27.0 kJ/mol, -46.2 kJ/mol, and -57.9 kJ/mol (or -61.5 kJ/mol from⁶⁵). However, these discrepancies have a clear physical explanation: it is well-known that π compounds may have a relatively strong interaction with metals of the Au group, notably Cu.⁶⁶ In particular, interactions with Au itself have also been recognized.⁶⁷ These originated by donation from the π electron cloud to surface atoms. Since the interaction is short-ranged, we devised a modified set of LJ gold parameters $\sigma'_{\text{AuAu}}/\sigma'_{\text{VS-VS}}$, $\epsilon'_{\text{AuAu}}/\epsilon'_{\text{VS-VS}}$ (to be combined via mixing rules with σ and ϵ of π C and H atoms), able to reproduce the experimental results for the three π -conjugated molecules. It is not obvious whether these LJ parameters should be assigned to virtual sites or to the real gold atoms (see Fig. 4). We found that experimental energies could be equally well reproduced by both choices (with different σ and ϵ , of course). The adsorption geometry is also qualitatively the same in both cases (molecular plane parallel to gold surface). What differs is the adsorption site: when only virtual sites are used, ethene adsorbs with the mid-point of the double bond on-top, and the center of the benzene ring coincides with the hollow site. Such results are reasonable: it is experimentally known that in ordered benzene monolayers, benzene molecules indeed occupy the hollow sites,⁶⁸ and the position of ethene, although not confirmed by experiments, is physically sound because on-top site is the more electrophilic. On the contrary, when LJ parameters are given to the real surface gold atoms (keeping the generic LJ on the virtual sites), the adsorption was not on high symmetry sites (i.e., no pure on-top, hollow or bridge site). Thus, we preferred to use special LJ parameters for virtual sites, keeping no LJ interaction

Table 4. Calculated and Experimental Interaction Energies With Special LJ Parameters for π Molecules.

Molecule	E_{FF} (kJ/mol)	E_{exp} (kJ/mol)
Ethene	−26.7	−27.0 ^a
1,3-Butadiene	−46.4	−46.2 ^a
Benzene	−60.3	−57.9 ^a , −61.5 ^b

^a[15].

^b[65].

with the real surface gold atoms. We found that $\sigma'_{\text{VS-VS}} = \sigma_{\text{VS-VS}} = 3.2 \text{ \AA}$ and $\epsilon'_{\text{VS-VS}} = 1.3125 \text{ kJ/mol}$ (to be used via OPLS mixing rules to obtain $\sigma'_{\text{VS-A}}$ and $\epsilon'_{\text{VS-A}}$) allow us to reproduce the experimental interaction energies well, as reported in Table 4.

To end this section, we present in Table 5 a summary of the FF parameters for easy reference. It can be useful to resume here on which data (computational/experimental) are the various parameters based. DFT results have been used in the first instance to probe the suitability of the FF used (they further confirmed the validity of the E_{image} term, already discussed in,²⁹ that dominates the adsorption energy for charged species), and then to provide the parameters for chemisorbed species ($E_{\text{chemisorb}}$). To fix the LJ parameters of gold and to verify the accuracy of mixing rules (in other words, to determine E_{vdW}), we have used experimental adsorption energy data of linear alkanes and performed *ab initio* MP2 calculations on model systems, respectively. The modified LJ parameters for π -molecules (E_{π}) have been obtained by experimental adsorption energy data.

Preliminary test of the FF

Validation of a FF is a long process that involves decades of applications and comparisons with experiments, so to put to the light the FF weaknesses and the necessary FF refinements. Benchmark experimental results for this validation process should be as clean and well-defined as possible. Ideal benchmarks would be well-characterized protein-gold (or at least peptide-gold) experi-

mental systems. Although experiments on gold binding peptides are available (including adsorption free energy¹⁴), MD simulations of such experiments remains a formidable computational task, due to the several unknown features of the experimental system at the microscopic level (just to cite a few: how is GBP oriented on the surface? how important are the inter-adsorbate interactions?) and some of its intrinsic properties (e.g., the conformational richness of GBP⁷⁰). We are presently working on such simulations, but they are beyond the scope of the present article. To show that this initial version of our FF is indeed reasonable, we tested a limited set of molecules different from that used to parameterize the FF (unfortunately the available experimental results for Au(111) are not many, and we used a good share of them to obtain parameters). We have considered cyclohexane, cyclooctane, acetone, diethylsulfide, trans-2-butene, toluene, 1-nonene, and 1-undecene, for which desorption energies are available. Cyclohexane and cyclooctane are alkanes, i.e., they share the same chemical nature with the LJ parameterization set. However, they have (rigid) geometries that are different from that of linear alkanes, and are good benchmark for geometric effects on the surface. Acetone contains a chemical functionality that was not specifically parameterized, so it is relevant to check the transferability of parameters. Diethylsulfide contains a chemical group (the sulfide) which has been parameterized via DFT calculations and other groups (the two ethyl moieties) whose parameters come from experiments. Trans-2-butene, toluene, 1-nonene, and 1-undecene mix two functionalities independently parameterized (π -bond and alkanes). The calculated interaction energies for all these species are reported in Table 6 and shown in Figure 8.

The agreement is remarkably good for all the considered molecules. The RMSD between calculation and experiment is 5 kJ/mol. For the longer alkenes (1-nonene and 1-undecene), FF results seem to overestimate the interaction energy. However, it has been recently argued⁷⁰ that for long alkanes experimental adsorption energies may be underestimated (in absolute value), from $\sim 10 \text{ kJ/mol}$ for octane to $\sim 25 \text{ kJ/mol}$ for dodecane. Such corrections are comparable with the discrepancy between the experimental values and our calculations. When these molecules are not considered, the RMSD decreases to 2.5 kJ/mol. We

Table 5. Summary of the GolP FF Parameters for Au(111).

	Int. site	$q(e)$	$\sigma_{\text{AuAu}}, \epsilon_{\text{AuAu}}^a$	$\sigma_{\text{AuAu}}, \epsilon_{\text{AuAu}}^b$	$\sigma_{\text{AuS}}, \epsilon_{\text{AuS}}^c$	$\sigma_{\text{AuN}}, \epsilon_{\text{AuN}}^d$	$\sigma_{\text{AuH}}, \epsilon_{\text{AuH}}^e$	Position ^f
Surface Au atom	2 AUI	0	3.2, 0.65	3.2, 1.3125	2.9, 2.7	2.75, 1.6	3.05, 0.5	(a/2, a/2 $\sqrt{3}$, 0)
	AUS	−0.3	0, 0	0, 0	0, 0	0, 0	0, 0	(−a/2, −a/2 $\sqrt{3}$, 0)
	AUC	0.3	0, 0	0, 0	0, 0	0, 0	0, 0	(0, 0, 0)
Bulk Au atom	AUB	−0.3	3.2, 0.65	0, 0	2.9, 2.7	2.75, 1.6	3.05, 0.5	0.7 Å from AUS
	AUC	0.3	0, 0	0, 0	0, 0	0, 0	0, 0	(0, 0, 0)
								0.7 Å from AUB

^aStandard OPLS mixing rules are used to find interactions with proteins and solvent atoms. σ in Å, ϵ in kJ/mol.

^bParameters to be combined via OPLS mixing rules for C and H of π systems.

^cFor S_{Met} and S_{Cys} , these over-rule the general parameters. σ in Å, ϵ in kJ/mol.

^dFor the unprotonated N_{His} and N_{NH_2} , these over-rule the general parameters. σ in Å, ϵ in kJ/mol.

^eOnly for H atoms of $-\text{NH}_2$.

^fThe real gold atom is at (0, 0, 0), a is the lattice constant (2.93 Å in our calculations) and the unit vectors for the surface cell are (1, 0, 0) and (1/2, $\sqrt{3}/2$, 0). AUC is constrained to be at a fixed distance from AUS (or AUB), but it is otherwise free to move ($m = 0.5 \text{ Da}$).

Table 6. Calculated and Experimental Interaction Energies for a Test Set of Molecules.

Molecule	E_{FF} (kJ/mol)	E_{exp} (kJ/mol)
Cyclohexane	−48.8	−50.6 ^a , −50 ^b
Cyclohexene	−51.4	−54 ^b
Cyclooctane	−60.8	−63.1 ^a
Acetone	−38.8	−41 ^c
Diethylsulfide	−68.4	−68 ^a
Toluene	−71.0	−66.1 ^a
Trans 2-butene	−41.1	−41.7 ^a
1-Nonene	−83.1	−76.2 ^a
1-Undecene	−99.3	−87.8 ^a

^a[15].^b[16].^c[17].

should also mention that an upper limit for the gold-water interaction has been estimated by Kay et al.,⁶⁴ and resulted to be −44 kJ/mol. Our calculated value is lower (−14 kJ/mol) and thus compatible with the experimental results.

The overall good agreement for this test set points to the reliability of the developed FF, although only an extensive application of the FF and the consequent comparison with the experiments can ultimately validate our work.

Conclusions

In this article, we have described the derivation of a FF to describe the interaction of proteins with the Au(111) surface. We employed a careful mixing of calculations and experimental data to work out a FF that is compatible with bio-oriented MD codes such as GROMACS and NAMD. Preliminary tests on small molecule adsorption on gold confirmed the reliability of the FF. The procedure used to parameterize gold did not only yield gold parameters, but it also set a protocol to be used for parameterizing other molecules on gold, or the same amino acids on other metals.

We would like to remark that the procedure to include image interaction is quite independent (at least for Au(III)) from the other aspects of the FF. In other words, other approaches to include image interaction effects, giving a similar description as ours, are compatible with the rest of our FF.

The description of charged surfaces to mimic electrochemical conditions is beyond the scope of the present work (although charge separation on the gold surface is already accounted for by GolP). It will be treated in future studies, by adding point charges on gold, and a neutralizing ion distribution in the simulation cell.

Acknowledgments

The authors thank Martin Höfling for helping with force field implementation in GROMACS, Arrigo Calzolari for helping in setting up the DFT calculations and Alessandra Catellani and the Prosurf team for useful discussions.

Appendix: Computational Details

PW-DFT Calculations: Generalities

PW-DFT calculations on molecules mentioned in Table 1 on Au(111) have been performed with the PWscf code included in the Quantum Espresso package.⁷¹ For all the molecules we used a $2\sqrt{3} \times 3$ supercell with four atomic layers of gold. Periodic boundary conditions in all the three Cartesian directions have been applied, with a thick vacuum layer to neutralize spurious interactions between neighboring replicas in the direction normal to the surface. All the calculations have been performed using the gradient-corrected PBE exchange-correlation functional,⁵⁵ with ultrasoft pseudo-potentials⁷² to describe electron-ion interactions. Plane waves up to a kinetic energy cutoff of 25 Ry for electron wave functions and 200 Ry for electron density were included in the basis set. A Gaussian smearing technique is used to deal with Brillouin zone integration.⁷³

PW-DFT Geometry Optimization

For geometry optimizations, the size of the periodic supercell in the direction perpendicular to the surface has been chosen so to have a vacuum thickness of 10 Å between the system and its closest replica. A $4 \times 4 \times 1$ Monkhorst-Pack k-point mesh was used for the Brillouin zone sums. For each molecule, structural relaxations were started by various initial geometries, differing for the relative positions of the molecule with respect to the gold lattice and for the orientation of the molecule in space. In this way, structures corresponding to distinct local minima could be identified. Among them, the lowest energy structure was identified and used for comparisons with classical results. All the atomic positions were relaxed until each atomic force component was smaller than 0.026 eV/Å.

PW-DFT Calculation of Adsorption Energies

Adsorption energies reported in Table 2 were calculated as the difference between the total energy of the optimized geometry of the molecule/gold system and the total energy of the system composed of a free molecule and a clean surface, simulated by placing the molecule at 10 Å from the surface, with the same orientation and in-plane location relative to the substrate as in the coupled interface. These total energies were computed at fixed optimized geometries with thicker supercells (containing 25 Å instead of 10 Å of vacuum) and with a finer $6 \times 8 \times 1$ Monkhorst-Pack k-point mesh than those used in structural relaxations, to increase the computational accuracy.

MP2 Calculations on the Interaction Energies Between $\text{Au}_4\text{-CH}_4$ and $\text{Au}_4\text{-H}_2\text{O}$

The geometry of the Au_4 cluster was obtained from a clean, unrelaxed Au slab used in PW-DFT calculations. HF and MP2 calculations of the interaction energies between $\text{Au}_4\text{-CH}_4$ and $\text{Au}_4\text{-H}_2\text{O}$ have been performed with the NWChem code⁷⁴ by using the DZP basis set and the Stuttgart effective core potential for Au. Basis set superposition errors have been corrected by the counterpoise method.⁷⁵

Generalities on Classical Simulations

All the classical calculations have been performed via Molecular Dynamics as implemented in GROMACS. The gold surface was represented by a gold slab with five layers. For neutral molecules, a $4\sqrt{3} \times 7$ supercell was employed. The supercell was 3D periodic, and the lattice constant in the direction perpendicular to the surface were at least 4 nm. For charged species, the very same super cell used in DFT calculations was also used for classical electrostatics. In fact, convergence of the total energy for charged (jellium-neutralized) cells is very slow with the cell size, and practically difficult to be reached. Thus, it is important to reproduce the same conditions in the classical calculations, so to have computationally comparable (although not physically converged) results. Constant volume was used for all the simulations. Water molecules were kept rigid with the SETTLE algorithm,⁷⁶ so to reproduce the most common situation for simulations of proteins in explicit water.

Electrostatics has been treated with the Particle Mesh Ewald approach (PME), with a 1.2 Å grid (tests with 1.0 Å showed no relevant differences) and a fourth order spline interpolation. LJ has been cut-off at $d = 11$ Å, with a smooth switching-off starting at $d = 10$ Å.

For all classical simulations, the same geometry of the gold slab as obtained from DFT calculations has been used. The orientation of the rod used to represent gold polarization were initially randomized, and a preliminary 50 ps MD simulations of the slab alone at $T = 300$ K (Nosé-Hoover^{77,78}) has been performed. The LINCS algorithm⁷⁹ was used to constrain the rod length during the simulations (parameters as in²⁹). The positions of real gold atoms were frozen during this initialization step and in any further dynamics.

Classical Minimum Energy Structure for Molecules on Au(111)

The method employed to reproduce image interactions requires that the gold rods should always be at finite temperature to give meaningful results. Thus, to obtain minimum energy structures for molecules on gold, we performed a simulated annealing MD simulation by using two different (Nosé-Hoover) thermostats: one applied to the gold slab with the temperature constantly held at 300 K, and one applied to the molecule to implement the annealing. We ran several annealing cycles for each molecule, starting from different arbitrarily chosen positions and orientations of the molecule inside the simulation cell. Each cycle had a duration of at least 40 ps (20 ps at $T = 300$ K, 15 ps of linearly descending ramp to $T = 1$ K and then 5 ps at 1 K). The non-electrostatic gold-molecule interaction energy has been calculated by taking the difference between the bond+angle+dihedral+LJ energy contribution for the structure resulting from the annealing and the minimized structure of the molecule without the metal.

Calculations of the Electrostatic Contribution

As described elsewhere,²⁹ the calculation of the electrostatic contribution should be done by estimating a *free-energy* electrostatic interaction energy between the molecule and the ensemble

of rods that model the gold slab. For neutral (or singly charged) molecules, this estimate can be performed by applying a linear response technique:

$$F_{\text{Coul}} = E_{\text{Coul}}/2 \quad (3)$$

where E_{Coul} is the gold-molecule electrostatic interaction energy averaged on the evolution of gold rods. Thus, after each annealing, a NVT simulation run (at least 50 ps, 500ps for charged molecules) was performed with the molecule fixed in the position obtained by the annealing and the gold rods free to move with $T = 300$ K.

References

1. Brown, S. *Proc Natl Acad Sci USA* 1992, 89, 8651.
2. Whaley, S. R.; English, D. S.; Hu, E. L.; Barbara, P. F.; Belcher, A. M. *Nature* 2000, 405, 665.
3. Sarikaya, M.; Tamerler, C.; Jen, A. K. -Y.; Schulten, K.; Baneyx, F. *Nature Mat* 2003, 3, 577.
4. (a) Carravetta, V.; Monti, S. *J Phys Chem B* 2006, 110, 6160; (b) Monti, S. *J Phys Chem C* 2007, 111, 16962–16973.
5. Mijajlovic, M.; Biggs, M. J. *J Phys Chem C* 2007, 111, 15839.
6. Cormack, A. N.; Lewis, R. J.; Goldstein, A. H. *J Phys Chem B* 2004, 108, 20408.
7. Tomasio, S. D.; Walsh, T. R. *Mol Phys* 2007, 105, 221.
8. Raffaini, G.; Ganazzoli, F. *Langmuir* 2003, 19, 3403.
9. Braun, R.; Sarikaya, M.; Schulten, K. *J Biomat Sci* 2002, 13, 747.
10. Makrodimitris, K.; Masica, D. L.; Kim, E. T.; Gray, J. J. *J Am Chem Soc* 2007, 129, 13713.
11. Horinek, D.; Serr, A.; Geisler, M.; Pirzer, T.; Slotta, U.; Lud, S. Q.; Garrido, J. A.; Scheibel, T.; Netz, R. R.; Hugel, T. *Proc Natl Acad Sci USA* 2008, 105, 2842.
12. Brown, S. *Nat Biotechnol* 1997, 15, 269.
13. Brown, S.; Sarikaya, M.; Johnson, E. *J Mol Biol* 2000, 299, 725.
14. Sarikaya, M.; Tamerler, C.; Schwartz, D. T.; Baneyx, F. *Annu Rev Mater Res* 2004, 34, 373.
15. Wetterer, S. M.; Lavrich, D. J.; Cummings, T.; Bernasek, S. L.; Scoles, G. *J Phys Chem B* 1998, 102, 9266.
16. Syomin, D.; Koel, B. E. *Surf Sci* 2002, 498, 61.
17. Syomin, D.; Koel, B. E. *Surf Sci* 2002, 498, 53.
18. Hautman, J.; Klein, M. L. *J Chem Phys* 1989, 91, 4994.
19. Hautman, J.; Bareman, J. P.; Mar, W.; Klein, M. L. *J Chem Soc Faraday Trans* 1991, 87, 2031.
20. Mar, W.; Klein, M. L. *Langmuir* 1994, 10, 188.
21. Pertsin, A. J.; Grunze, M. *Langmuir* 1994, 10, 3668.
22. Sellers, H.; Ulman, A.; Shnidman, Y.; Eilers, J. E. *J Am Chem Soc* 1993, 115, 9389.
23. Vemparala, S.; Karki, B. B.; Kalia, R. K.; Nakano, A.; Vashishta, P. *J Chem Phys* 2004, 121, 4323.
24. Sadreev, A. F.; Suhunin, Y. V.; Petoral, R. M.; Uvdal, K. *J Chem Phys* 2004, 120, 954.
25. Spohr, E. *J Mol Liq* 1995, 64, 91.
26. Dou, Y.; Zhigilei, L. V.; Winograd, N.; Garrison, B. J. *J Phys Chem A* 2001, 105, 2748.
27. Qian, J.; Hentschke, R.; Knoll, W. *Langmuir* 1997, 13, 7092.
28. Rappè, A. R.; Casewit, C. J.; Colwell, K. S.; Goddard, W. A., III; Skiff, W. M. *J Am Chem Soc* 1992, 114, 100210.
29. Iori, F.; Corni, S. *J Comp Chem* 2008, 29, 1656.
30. Schravendijk, P.; van der Vegt, N. F. A.; Delle Site, L.; Kremer, K. *Chem Phys Chem* 2005, 6, 1866.

31. Tupper, K. J.; Brenner, D. W. *Langmuir* 1994, 10, 2335.
32. Mahaffy, R.; Bhatia, R.; Garrison, B. J. *J Phys Chem B* 1997, 101, 771.
33. (a) Stave, M. S.; Sanders, D. S.; Raeker, T. J.; DePristo, A. E. *J Chem Phys* 1990, 93, 4413; (b) Raeker, T. J.; DePristo, A. E. *Int Rev Phys Chem* 1991, 10, 1; (c) Kelchner, C. L.; Halstead, D. M.; Perkins, L. S.; Wallace, N. M.; DePristo, A. E. *Surf Sci* 1994, 310, 425.
34. Gerdy, J. J.; Goddard, W. A., III. *J Am Chem Soc* 1996, 118, 3233.
35. Mayo, S. L.; Olafson, B. D.; Goddard, W. A., III. *J Phys Chem* 1990, 94, 8897.
36. Zhang, L.; Goddard, W. A., III; Jiang, S. *J Chem Phys* 2002, 117, 7342.
37. Jang, S. S.; Jang, Y. H.; Kim, Y. H.; Goddard, W. A.; Flood, A. H.; Laursen, B. W.; Tseng, H. R.; Stoddart, J. F.; Jeppesen, J. O.; Choi, J. W.; Steuerma, D. W.; Delonno, E.; Heath, J. R. *J Am Chem Soc* 2005, 127, 1563.
38. Dirama, T. E.; Johnson, J. A. *Langmuir* 2007, 23, 12208.
39. (a) Baxter, R. J.; Teobaldi, G.; Zerbetto, F. *Langmuir* 2003, 19, 7335; (b) Rapino, S.; Zerbetto, F. *Langmuir* 2005, 21, 2512.
40. Rappè, A. K.; Goddard, W. A., III. *J Phys Chem* 1991, 95, 3358.
41. Ercolessi, F.; Parrinello, M.; Tosatti, E. *Philos Mag A* 1998, 58, 213.
42. Teobaldi, G.; Zerbetto, F. *J Phys Chem C* 2007, 111, 13879.
43. Leng, Y.; Keffer, D. J.; Cummings, P. T. *J Phys Chem B* 2003, 107, 11940.
44. Bizzarri, A. R.; Costantini, G.; Cannistraro, S. *Biophys Chem* 2003, 106, 111.
45. Setty-Venkat, A.; Corni, S.; Di Felice, R. *Small* 2007, 8, 1431.
46. Piana, S.; Bilic, A. *J Phys Chem B* 2006, 110, 23467.
47. (a) Finnis, M. W.; *Surf Sci* 1991, 241, 61; (b) Finnis, M. W.; Kaschner, R.; Kruse, C.; Furthmüller, J.; Scheffler, M. *J Phys Condens Matter* 1995, 7, 2001.
48. Siepmann, J. I.; Sprik, M. *J Chem Phys* 1995, 102, 511.
49. Spohr, E. *J Electroanal Chem* 1998, 450, 327.
50. van der Spoel, D.; Lindahl, E.; Hess, B.; Groenhof, G.; Mark, A. E.; Berendsen, H. J. C. *J Comp Chem* 2005, 26, 1701.
51. Phillips, J. C.; Braun, R.; Wang, W.; Gumbart, J.; Tajkhorshid, E.; Villa, E.; Chipot, C.; Skeel, R. D.; Kale, L.; Schulten, K. *J Comp Chem* 2005, 26, 1781.
52. Dick, B. G.; Overhauser, A. W. *Phys Rev* 1958, 112, 90.
53. Lamoureux, G.; Roux, B. *J Chem Phys* 2003, 119, 3025.
54. Perdew, J. P.; Burke, K.; Ernzerhof, M. *Phys Rev Lett* 1996, 77, 3865.
55. Michaelides, A.; Ranea, V. A.; de Andres, P.L.; King, D. A. *Phys Rev Lett* 2003, 90, 216102.
56. Di Felice, R.; Selloni, A. *J Chem Phys* 2006, 120, 4906.
57. Bilic, A.; Reimers, J. R.; Hush, N. S.; Hafner, J. *J Chem Phys* 2002, 116, 8981.
58. Iori, F.; Corni, S.; Di Felice, R. *J Phys Chem C* 2008, 112, 13540.
59. Brenner, D. W. *Phys Rev B* 1990, 42, 9458.
60. van Duin, A. C. T.; Dasgupta, S.; Lorant, F.; Goddard, W.A., III. *J Phys Chem A* 2001, 105, 9396.
61. Müller, J. E. *Appl Phys A* 2007, 87, 433.
62. Righi, M. C.; Ferrario, M. *J Phys Condens Matter* 2007, 19, 305008.
63. Kaminski, G. A.; Friesner, R. A.; Tirado-Rives, J.; Jorgensen, W. L. *J Phys Chem B* 2001, 105, 6474.
64. Kay, B. D.; Lykke, K. R.; Creighton, J. R.; Ward, S. J. *J Chem Phys* 1989, 91, 5120.
65. Syomin, D.; Kim, J.; Koel, B. E.; Ellison, G. B.; *J Phys Chem B* 2001, 105, 8387.
66. Ferretti, A.; Baldacchini, C.; Calzolari, A.; Di Felice, R.; Ruini, A.; Molinari, E.; Betti, M. G. *Phys Rev Lett* 2007, 99, 046802.
67. Schroeder, P. G.; France, C. B.; Park, J. B.; Parkinson, B. A. *J Phys Chem B* 2003, 107, 2253.
68. Han, P.; Mantooth, B. A.; Sykes, E. C. H.; Donhauser, Z. J.; Weiss, P. S. *J Am Chem Soc* 2004, 126, 10787.
69. Kulp, J. L.; Sarikaya, M.; Evans, J. S. *J Mater Chem* 2004, 14, 2325.
70. Fichthorn, K. A.; Becker, K. E.; Miron, R. A. *Catalysis Today* 2007, 123, 71.
71. Baroni, S.; Dal Corso, A.; de Gironcoli, S.; Giannozzi, P. Available at: <http://www.pwscf.org>
72. Vanderbilt, D. *Phys Rev B* 1990, 41, 7892.
73. Fu, C.-L.; Ho, K.-M. *Phys Rev B* 1983, 28, 5480.
74. Straatsma, T. P.; Aprà, E.; Windus, T. L.; Bylaska, E. J.; de Jong, W.; Hirata, S.; Valiev, M.; Hackler, M.; Pollack, L.; Harrison, R.; Dupuis, M.; Smith, D. M. A.; Nieplocha, J.; Tipparaju V.; Krishnan, M.; Auer, A. A.; Brown, E.; Cisneros, G.; Fann, G.; Früchtl, H.; Garza, J.; Hirao, K.; Kendall, R.; Nichols, J.; Tsemekhman, K.; Wolinski, K.; Anchell, J.; Bernholdt, D.; Borowski, P.; Clark, T.; Clerc, D.; Dachsel, H.; Deegan, M.; Dyall, K.; Elwood, D.; Glendenning, E.; Gutowski, M.; Hess, A.; Jaffe, J.; Johnson, B.; Ju, J.; Kobayashi, R.; Kutteh, R.; Lin, Z.; Littlefield, R.; Long, X.; Meng, B.; Nakajima, T.; Niu, S.; Rosing, M.; Sandrone, G.; Stave, M.; Taylor, H.; Thomas, G.; van Lenthe, J.; Wong, A.; Zhang, Z.; NWChem, A Computational Chemistry Package for Parallel Computers, Version 4.6 (2004), Pacific Northwest National Laboratory, Richland, Washington 99352-0999, USA. High Performance Computational Chemistry: an Overview of NWChem a Distributed Parallel Application, Kendall, R.A.; Aprà, E.; Bernholdt, D.E.; Bylaska, E.J.; Dupuis, M.; Fann, G.I.; Harrison, R.J.; Ju, J.; Nichols, J.A.; Nieplocha, J.; Straatsma, T.P.; Windus, T.L.; Wong, A.T. *Computer Phys Commun* 2000, 128, 260.
75. Boys, S.F.; Bernardi, F. *Mol Phys* 1970, 19, 553.
76. Miwamoto, S.; Kollman, P. A. *J Comp Chem* 1992, 13, 952.
77. Nosè, S. *Mol Phys* 1984, 52, 255.
78. Hoover, W. G. *Phys Rev A* 1985, 31, 1695.
79. Hess, B.; Bekker, H.; Berendsen, H. J. C.; Fraaije, J. G. E. M. *J Comp Chem* 1997, 18, 1463.